arXiv:1403.5631v1 [astro-ph.IM] 22 Mar 2014

An analytical approach to optimize AC biasing of bolometers

Andrea Catalano,[1,2,*] Alain Coulais,[2] Jean-Michel Lamarre[2]

[1] *Laboratoire AstroParticule et Cosmologie (APC), Université Paris Diderot, CNRS/IN2P3, Observatoire de Paris, 10, rue Alice Domon et Léonie Duquet, 75205, Paris cedex 13, France*

[2] *LERMA, Observatoire de Paris et CNRS, 61 Avenue de l'Observatoire, 75014 Paris, France*

[*] *Corresponding author: catalano@apc.univ-paris7.fr*

Bolometers are most often biased by Alternative Current (AC) in order to get rid of low frequency noises that plague Direct Current (DC) amplification systems. When stray capacitance is present, the responsivity of the bolometer differs significantly from the expectations of the classical theories. We develop an analytical model which facilitates the optimization of the AC readout electronics design and tuning. This model is applied to cases not far from the bolometers in the Planck space mission. We study how the responsivity and the NEP (Noise Equivalent Power) of an AC biased bolometer depend on the essential parameters: bias current, heat sink temperature and background power, modulation frequency of the bias, and stray capacitance. We show that the optimal AC bias current in the bolometer is significantly different from that of the DC case as soon as a stray capacitance is present due to the difference in the electro-thermal feedback. We also compare the performance of square and sine bias currents and show a slight theoretical advantage for the last one. This work resulted from the need to be able to predict the real behaviour of AC biased bolometers in an extended range of working parameters. It proved to be applicable to optimize the tuning of the Planck High Frequency Instrument (HFI) bolometers.

© 2014 Optical Society of America

OCIS codes: 000.0000, 040.0040.

1. Introduction

Bolometers are now the most sensitive receivers for astrophysical observations in the submillimetre spectral range. After decades of improvement, they are able to operate with a sensitivity limited by the photon noise of the observed source when operated outside of the atmosphere [1]. The principle of a bolometer is that the heat deposited by the incoming radiation is measured by a thermometer. The theory of bolometers has been developed in founding papers [2] and refined later [3–5]. They have shown that their photometric responsivity strongly depends on its interaction with the readout electronics, through the variation of the electrical power deposited in the thermometer (the electro-thermal feedback). These theories have been developed for a semiconductor thermometer element biased by a Direct Current (DC) voltage through a load resistor. The readout electronics for bolometers experienced a radical change more than a decade ago. Most of them are now using a modulated bias current in order to get rid of low frequency noises that plague amplification systems [6–10].

The theory developed for a DC bias must be altered for Alternative Current (AC) biased bolometers in the presence of stray capacitance in the circuit. This was evidenced in the Planck-HFI instrument [11] in spite of the fact that the readout electronics had been designed [9] to mimic, as far as possible, the operation of a DC bias. Very significant differences were found in absolute responsivity and even in value of the optimal bias current for the Planck bolometers. This was shown to be mostly due to the effect of parasitic capacitances in the wiring, which cannot be neglected in many practical experimental setups. This effects have been studied in several papers dedicated to the characterization of bolometers and calorimeters by measuring their effective impedance (e.g. [12]), but we are here essentially interested in effective tools able to predict the responsivity and optimise the tuning of bolometers in specific configurations. Brute force modelling based on numerical integration of thermal and electrical equations of the bolometers proved to be feasible but computationally too heavy to be applied on wide ranges of the many parameters of the models. To facilitate the computation, we have developed an analytical model of the responsivity of AC biased semiconductor bolometers. This model was used as an aid to predict the behaviour of the bolometer of Planck-HFI and to optimize their tuning. Its numerical application proved to be flexible and fast enough to study the effects of all variable parameters.

This paper describes this analytical model and its application with a set of parameters not too far from the realistic cases encountered in Planck-HFI. The next section is dedicated to the differential equations driving the thermal and the electrical behaviour of the electro-thermal system comprising the bolometer and its readout electronics. It focuses on the derivation of an analytical solution giving the responsivity for both the DC and AC biased cases. Section three addresses the various noises encountered and shows that the optimal bias currents are different in the two cases. In the fourth section the model is applied

to analyze the effects of some essential parameters (cold stage temperature, modulation frequency, value of the stray capacitance, optical background). Section five deals with the shape of the periodic bias wave to cover the case of square bias current used in Planck-HFI.

2. The Theoretical Model

2.A. Bolometer Model

Let us consider a low temperature bolometer consisting of an absorber attached to a semiconductor thermometer. The bolometer is attached to a heat sink at temperature T_0 through a thermal link of thermal conductance G_s. The incoming optical power deposits energy in the absorber and heats the whole bolometer including the thermometer. The absorbed optical power will determine the equilibrium temperature T_b of the bolometer:

$$G_s(T_b - T_0) = W_{tot} \tag{1}$$

Where W_{tot} is the total power dissipated in the bolometer that is $W = P + Q$ where Q is the absorbed radiant power and $P(t) = V(t)I(t)$ is the electrical power.

G_s can be well represented in many cases by:

$$G_s = G_{s0}(T_b/T_0)^{\beta}$$

where G_{s0} is the static thermal conductance at temperature T_0 ($100mK$ in the case we investigate here).

The dominant electrical conduction mechanism in the thermometer is the variable range hopping between localised sites and the resistance of the device varies with both applied voltage and temperature.

The relation between the resistance and the temperature of the bolometer [13] is set by :

$$R(T, E) = R_* exp\left(\left(\frac{T_g}{T}\right)^n - \frac{eEL}{K_b T}\right) \tag{2}$$

where T_g is a characteristic parameter of the material, R_* is a parameter depending on the material and the geometry of the element, L is related to the average hopping distance and E is the electric field across the device. In absence of electrical non-linearities and other effects such as electron-phonon decoupling, the thermistor resistance depends only on temperature:

$$R(T) = R_* exp\left(\frac{T_g}{T}\right)^n \tag{3}$$

The impedance changes induced by the temperature variations can be measured by an appropriate readout circuit that we are going to detail and discuss hereafter.

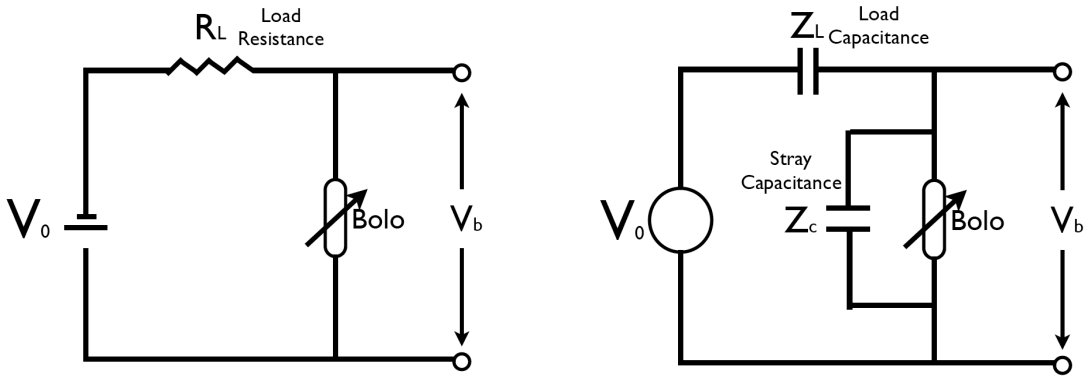

Fig. 1. Schemes of a DC (left) and an AC (right) bias circuits

2.B. Readout Electronics

The Readout Electronics is designed to measure the impedance of the temperature sensitive element of the bolometer. This is done by injecting a current, and therefore depositing power in the bolometer, which changes its temperature. Consequently, the bolometer responsivity and performance strongly depend on the design of the readout electronics.

The Responsivity $\Re$ is the derivative of the bolometer voltage with respect to the optical absorbed power W:

$$\Re = \frac{dV}{dW} \tag{4}$$

It is a strong indicator of the coupling efficiency achieved by readout electronics for a given bolometer.

We compare here after the responsivity obtained with a classical DC bias and a sine-shape AC bias.

DC Responsivity : the bolometer is biased with a DC bias voltage through a load resistance R_L, and the voltage V_b is measured with an amplifier with an high input resistance (Fig 1 left). The general equation of a DC biased circuit is :

$$V_b^{DC} = \frac{R_b}{R_b + R_L} V_0 \tag{5}$$

where R_L and R_b are the impedances of the load and the bolometer. V_0 is the total input voltage.

The electrical responsivity $\Re_{el}$ can be written using the Zwerling formalism [14]

$$\Re_{el} = \frac{\alpha \varphi_{DC} R_b I_b}{G_e} \tag{6}$$

where :

$$\varphi_{DC} = \frac{R_L}{R_b + R_L}$$

and G_e is the equivalent thermal conductance :

$$G_e = G_{s0} - \alpha R_b I_b^2 (2\varphi_{DC} - 1) \tag{7}$$

α is the temperature coefficient of resistance of the bolometer :

$$\frac{dR_b}{dT_b} = \alpha \cdot R_b \tag{8}$$

The advantage of this DC setup is the use of a well established theory [2, 3]. The optical power W_{opt} absorbed by the bolometer and the responsivity of the bolometer can be directly computed in the time domain. On the other hand, a DC bias current increases the level of low frequency noise, like Flicker noise, making the detection of a faint and slowly varying optical signal impossible. In addition, the Johnson noise produced by the load resistor forces us to put this element on the coldest cryogenic stage.

AC Responsivity: Let us consider now an AC bias circuit as presented in Fig. 1 right. The voltage at the ends of bolometer is:

$$V_b^{AC} = V_0 \cdot \frac{R_b Z_c}{Z_L Z_c + R_b (Z_L + Z_c)} \tag{9}$$

If we assume that the AC bias frequency F_{mod} is much higher than the bolometer cut-off frequency ($F_{mod} >> \frac{G_e}{2\pi C}$), then we can consider only the average electrical power and a steady state responsivity and neglect short term variations. We can derive a modified Zwerdling's formula for the responsivity by following the method used in the previous section for a DC biased bolometer:

$$\Re_{el} = \frac{\alpha \varphi_{AC} R_b I_b}{G_e^{AC}} \tag{10}$$

where G_{AC} the dynamic thermal conductance is equal to:

$$G_e^{AC} = G_s + \frac{dG_s}{dT}(T - T_0) - \alpha R_b I_b^2 (2\varphi_{AC} - 1) \tag{11}$$

Here the φ_{AC} factor is:

$$\varphi_{AC} = \frac{Z_L Z_c}{Z_L Z_c + R_b (Z_L + Z_c)} \tag{12}$$

where, if Z_L is a resistor:

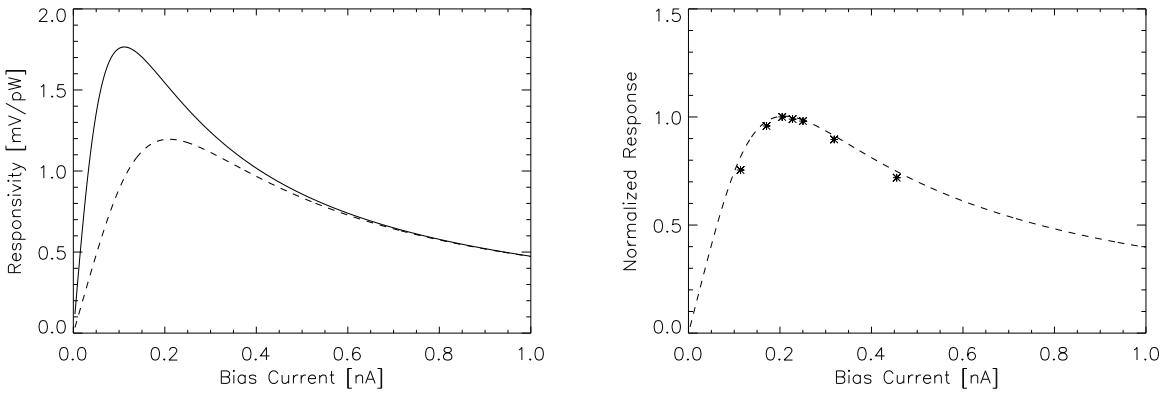

Fig. 2. Left: Simulation of responsivity versus bias current in the bolometer for DC (solid curve) and AC sine (dashed curve) bias currents in the case of a 3 mm bolometer (using parameters from Tab. 1). For AC model we consider a sine wave bias with a stray capacitance of $C_p = 130$ pF and plot the responsivity versus the r.m.s. value of the bias current. Right: Consistency of the AC model (dashed curve) with experimental measurements (stars points) taken from ground calibration of Planck HFI. The disagreement is of the order of 1 %.

$$\lim_{Z_c \to \infty} \varphi_{AC} = \varphi_{DC}$$

If we consider the module of the φ factor we can plot (Fig. 2) a responsivity versus bias current for DC and AC currents (sine-shape) bolometer. We can conclude that in terms of responsivity a DC electronics is preferable. For an AC bias the maximum in responsivity is lower and is obtained with higher bias current in the bolometer. We show in the next section that for slowly varying signals, AC bias has a decisive advantage in sensitivity.

3. Noise

The Noise Equivalent Power (NEP) is:

$$NEP(f) = \frac{< \Delta S^2(f) >^{1/2}}{\Re(f)} \tag{13}$$

where ΔS^2 is the power spectral density of the noise and $\Re$ is the responsivity of the detector. NEP is measured in $[W/Hz^{1/2}]$.

In our model we take into account all the principal sources of noise in bolometric detection: Johnson noise, phonon noise, photon noise, Flicker noise and the preamplifier noise. The

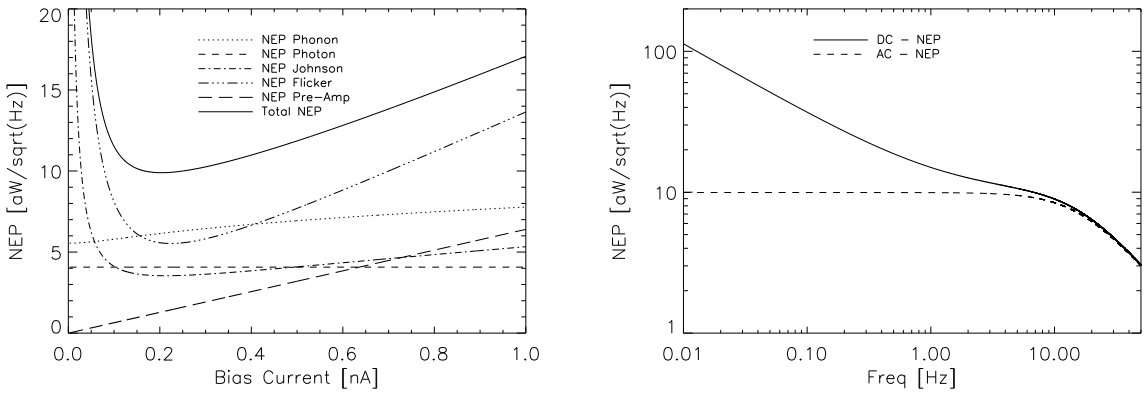

Fig. 3. Left: noise equivalent power versus bias current in the bolometer for different sources of noise in case of an AC readout electronics for the test bolometer $\lambda = 3$ mm. Right: total NEP versus frequency for a DC and AC readout electronics at respective best bias currents.

following is a review of the NEPs for the different sources of noise existing in literature (see for instance [3, 15]) :

Johnson noise: Johnson noise is the electronic noise generated by the thermal agitation of electrons inside a bolometer at equilibrium. It has a white noise spectrum. The NEP for DC biased bolometers is [3]:

$$NEP_{john} = (4k_B T_b R_b I_b^2)^{1/2} \frac{|Z_b + R_b|}{|Z_b - R_b|} \tag{14}$$

where R_b is the bolometer resistance and Z_b is its dynamic impedance.

Let us notice with Mather [3] that Johnson noise does not depend on load impedance. Let us assume here that it does not depend on stray capacitance in the case of AC biased bolometers. Hereafter, we shall use Eq. 14 indifferently with a DC model or an AC Model.

Phonon noise: The parameters of the bolometer are strongly dependent on the temperature, so small variations in temperature inside the bolometer produce a voltage variation at the ends of the detector.

It results [3]:

$$NEP_{phon} = (4k_B G T^2)^{1/2} \tag{15}$$

This result is independent of the readout electronics.

Photon noise: The Photon noise comes from the fluctuations of the incident radiation due to the Bose-Einstein distribution of the photon emission. The NEP is [15]:

$$NEP_{phot} = 2 \int_{\Delta\nu} h\nu Q_\nu d\nu + (1 + P^2) \int_{\Delta\nu} \Delta(\nu) Q_\nu^2 d\nu \tag{16}$$

Where Q_ν is the absorbed optical power per unit of frequency, $\Delta(\nu)$ is the coherence spacial factor (equal to the inverse of the number of modes; $\Delta(\nu) = 1$ if diffraction limited) and P is the polarisation degree (0 non-polarised 1 polarised). This noise corresponds to the limitation in sensitivity of any instrument because it does not depends on performances of detectors and readout electronics.

Flicker noise: The Flicker noise depends on a distribution of time constants due to the recombination and generation phenomena appearing in semiconductors.

This noise shows a spectrum directly proportional to the bias current and inversly proportional to the frequency. To first order we have :

$$NEP_{fl} = const \frac{I_b}{\sqrt{freq}} \tag{17}$$

The Flicker noise is usually the dominant source of noise up to few Hertz. In the case of AC electronics, we can choose the working modulation frequency in order to keep the Flicker noise less then the photon noise (see Fig. 3 right).

Preamplifier noise: results from the impossibility to amplify a signal without adding noise, which is a consequence of the Heisenberg Uncertainty principle. It also depends on the available components and on the design of the amplifier. We assume that the power spectrum of signal fluctuation is constant and equal to:

$$< \Delta S^2 >_{pre}^{1/2} = const = \sigma_{PA}[V/Hz^{1/2}]$$

The NEP_{pre} results from Eq. 13 as:

$$NEP_{pre} = \frac{\sigma_{PA}}{\Re} \tag{18}$$

The Total NEP of the instrument is:

$$NEP_{tot} = \left[NEP_{john}^2 + NEP_{phon}^2 + NEP_{phot}^2 + NEP_{fl}^2 + NEP_{pre}^2\right]^{1/2} \tag{19}$$

Fig. 3 (left) presents the influence of the different contributions to the total NEP for an AC readout electronics.

Fig. 3 (right) shows the advantage of using of an AC system instead of a DC solution at low frequencies. It is clear that Flicker noise increases the DC total NEP at low frequencies making the AC solution mandatory for the measurement of low and very low frequency signals (less then few Hertz).

Optimization of the Bias Current : from Fig. 2 it is clear that in both cases (AC and DC), the responsivity strongly depends on the bias current in the bolometer. The optimisation of this parameter is therefore a key point. We want to present a general result, not depending on the preamplifier noise level. Since our practice and all the simulations (see Fig.

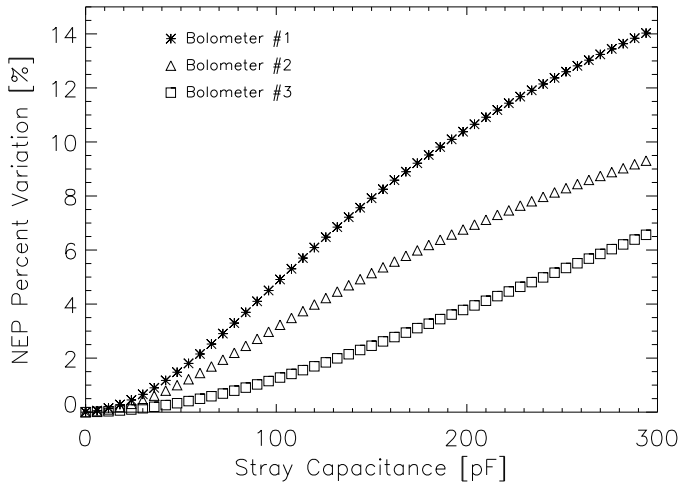

Fig. 4. Relative variation of the total NEP versus stray capacitance from 0 to 300 pF for three typical bolometers with an AC sine bias.

3) show that the minimum NEP happens very near to the maximum responsivity (to better than 1% in practical cases), we have chosen to use the responsivity to illustrate this point. The amplitude and the position of the peak responsivity are different for the two types of bias current. In the case presented in Fig. 2, the bias currents corresponding to the maximum of the Responsivity are equal to $I_{best}^{DC} = 0.12$ nA and $I_{best}^{AC} = 0.22$ nA.

4. Variation of Responsivity with Readout Electronics and Environmental Parameters

We are now interested in establishing the performance of AC readout electronics biased with a sine wave. We will derive the responsivity, the NEP and how the NEP depends on the main parameters (stray capacitance, modulation frequency, optical background and plate temperature) for three typical bolometers optimized to observe the sky between 0.3 and 3 mm cooled to a temperature of 100 mK. In order to obtain an analytical solution to this problem, we developed a model in the frequency domain using the Fourier formalism. The results could be also obtained in the case of a square AC model. The two methods are detailed in the appendices A and B.

4.A. Stray Capacitance

The first stage of preamplifiers for semiconductors bolometers are classically J-FETs giving optimal performance at 100 K or more. Rather long wiring is needed between the J-FETs

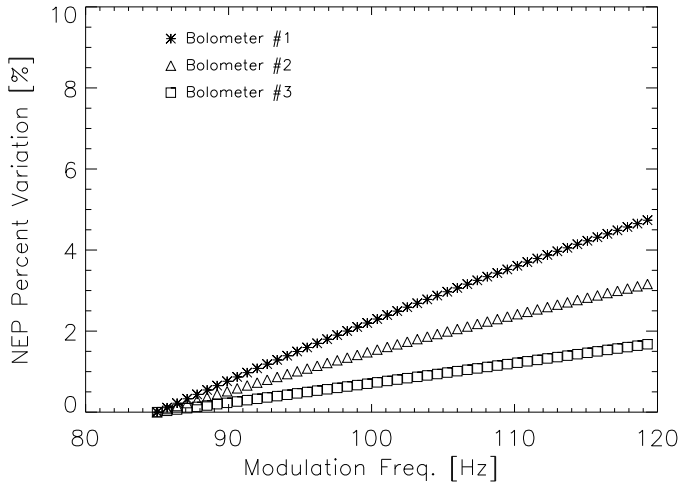

Fig. 5. Relative variation of the total NEP versus modulation frequency of the AC sine from 85 Hz to 120 Hz for three typical bolometers

and the bolometer to avoid an excessive thermal load on the sub-Kelvin stage supporting the bolometer. Stray capacitance of tens and even hundreds of picoFarads result from this design. In Fig. 4, we plot for our three test bolometers the excess of NEP versus the value of the stray capacitance. For a typical value of 150 pF, the NEP excess is several percents (from 4 % to 8 %). Let us note here that the DC bias case is identical to an AC case without stray capacitance.

4.B. Modulation Frequency

As we have seen in previous section, the use of an AC bias has the advantage of presenting a noise spectrum flat down to very low frequencies, while DC biased readouts show a large 1/f component at frequencies less than about 10 Hz. The modulation frequency of the electronics will be chosen therefore taking into account the requirement of keeping the Flicker noise less then the Johnson noise but also taking into account the scanning strategy of the instrument and the angular responsivity of the optics. In the case of Planck HFI for example [11] the full width at half maximum δ ranges from 5 to 9 arcmin and the scanning speed is 6 degrees per second. So, in the limit of small angles, the maximum frequency of interest is given by the relation:

$$f \sim \frac{v_{ang}}{\delta} \tag{20}$$

where f is the frequency of the optical modulation. In Fig. 5 we consider the excess NEP

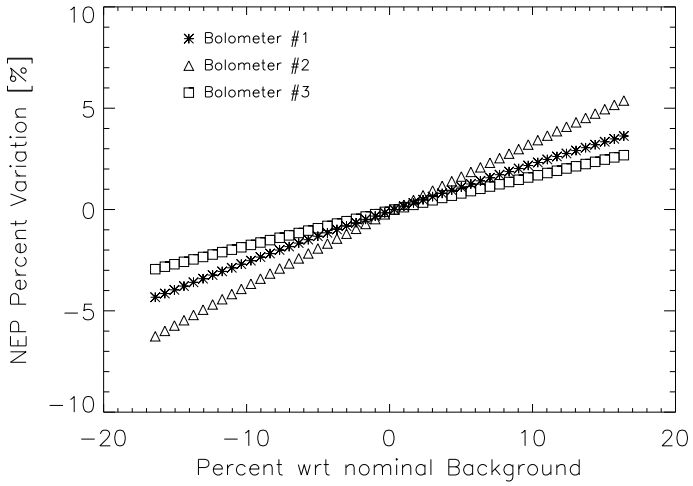

Fig. 6. Relative variation of the total NEP versus optical background. We consider for each bolometer a total range in background equal to 33 % of the nominal background.

with respect to a 85 Hz modulation frequency. In the worst case the excess NEP is 0.5 % per Hertz.

4.C. Optical Background

The background strongly affects the static performance of a bolometer by changing the operating point. With respect to others parameters, the background is the most uncertain and variable parameter during an observational campaign. A good understanding of the effect of the optical background on the static performances of a bolometers is therefore a key point during the calibration of the instrument. In Fig. 6 we present the relative variation of the total NEP versus the nominal background for our test bolometers. For the 3 mm bolometer, the nominal background is 0.3 pW; for 1 mm 0.6 pW and for 0.3 mm 3.6 pW. In the worst case the degradation in NEP is 2 % with respect the nominal background for a background increase of +16.5 %.

4.D. Bolometer Plate Temperature

Following the first order thermal model of a bolometer (Eq. 1), we know that a change in temperature of the plate corresponds exactly to a change of background power on the bolometer. In this case the equivalent power generated from a change of the plate temperature is:

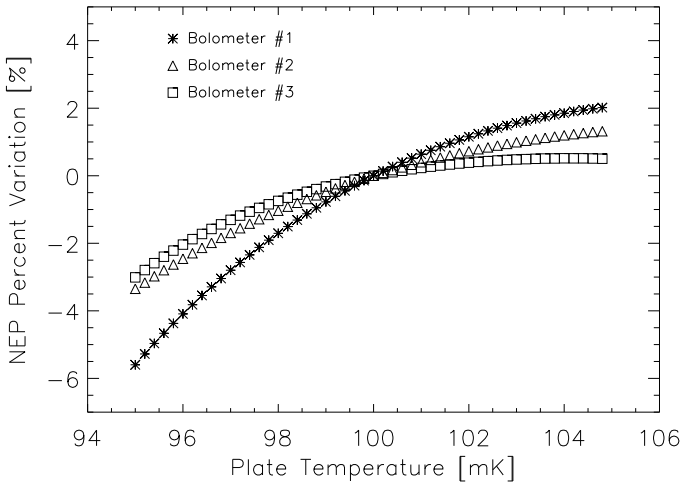

Fig. 7. Relative variation of the total NEP versus bolometer plate temperature from 95 mK to 105 mK for the three test bolometers.

$$\Delta P_{plate} = G_s \Delta T_0 \tag{21}$$

Our test bolometers were designed for a plate temperture of 100 mK. The NEP variation in the range 95 mK – 105 mK is reported in Fig. 7. We find that a change of the plate temperature of 1 mK gives a change in NEP of 0.8 % in the worst case.

5. Comparison Between two Modulation Techniques : Sine AC Bias vs Square AC Bias

We want now to compare the performances, in terms of responsivity and NEP, of a sine-wave and a square-wave AC electronics. The results are shown in Fig. 8. The sine case is better for both responsivity and NEP. This is more obvious for the responsivity (better by about 10 %) than for the total NEP (better by about 4 %). We conclude that in terms of NEP, a bolometer connected to a sine AC biased readout electronics would be more sensitive.

Let us remark that the difference in NEP is modest. Let us also notice that an AC sine bias would induce significant variations in the temperature of the fastest bolometers, bringing them into the non-linear regime. On the contrary, the square bias deposits a nearly constant power in the bolometers, that deviate from their mean temperature only by small amounts.

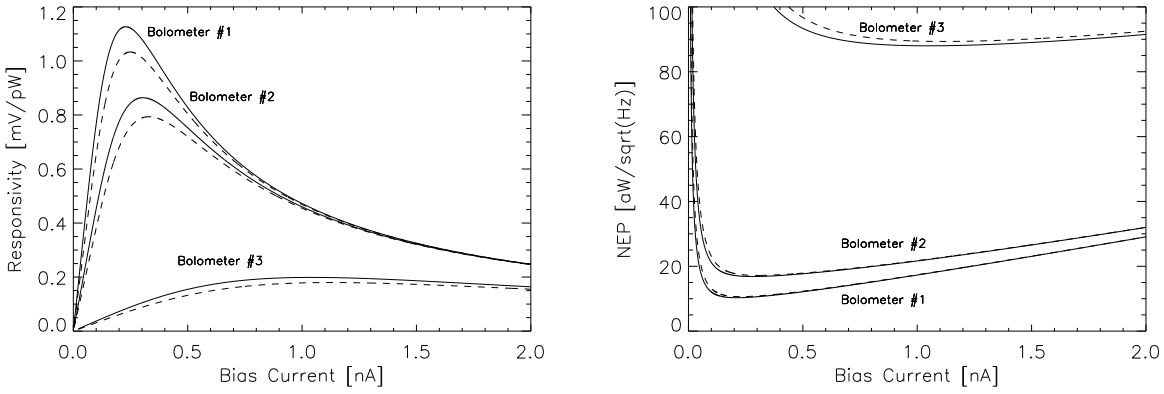

Fig. 8. Simulation of responsivity (left) and total NEP (right) of the three test bolometers in case of an AC sine bias (solid curves) and a square AC bias (dashed curves)

	wavelength	$R_*[Ohm]$	$G_{so}[pW/K]$	$T_g[K]$	n	β
Bolo #1	3 mm	100	52	16	0.5	1.3
Bolo #2	1 mm	94	70	16	0.5	1.3
Bolo #3	0.3 mm	105	703	16.5	0.5	1.1

Table 1. *Parameters of the test bolometers used to illustrate the results of the analytical model.*

6. Conclusion

The analytical model presented in this paper has been developed for the HFI on board Planck satellite. It allowed us to predict the responsivity and the noise of semi-conductor bolometers cooled at 100 mK and biased by AC currents in a realistic environment. It sheds some light on the differences between AC and DC biased bolometer and on the different optimal bias currents for these two cases. Three test bolometers rather similar to Planck's ones were used to illustrate our results. Our main conclusions are:

- The AC responsivity is always lower than the DC responsivity. This is due to a more effective electro-thermal feedback. The resulting excess of NEP depends on the relative part of the preamplifier noise in the total NEP. In our test cases the excess NEP ranges from 4 % to 10 %, which is more than compensated for by shifting of the low frequency noises out of the range of useful frequencies. Frequencies down to 1 mHz are measurable

with a well designed AC readout electronics.

- The AC bias RMS current providing to the maximum of the responsivity is about twice larger than that obtained for a DC bias. This concerns the current through the bolometer and results from the different electro-thermal feedback.
- For a stray capacitance of $\sim$ 150 pF we obtain an excess NEP of 10 % in the worst case (3 mm bolometer) and 4% in the best case (0.3 mm bolometer).
- Around a modulation frequency of 90 Hz, the excess NEP ranges between 0.2 % and 0.5 % per Hz.
- The sensitivity of NEP to background is dlog(NEP)/dlog(Wbg) = 0.22 to 0.42
- The sensitivity of NEP to the plate temperature is dlog(NEP)/dlog(Tplate) = 0.3 to 0.8 around 100 mK, but is rather non-linear.
- The performances of a sine bias are better than the square bias. In our test cases, this result is more obvious in the responsivity (better by about 10 %) than in the total NEP (better by about 4 %). But non-linear effects may show up in the sine case for bolometers fast enough to respond to the modulation frequency.

Appendix A: Computing the Responsivity with a Sine Bias

Let us consider the bias circuit of Fig. 1 with a stray capacitance in parallel to the bolometer and a load capacitance in series. The value of the load capacitance is fixed to $C_b = 4.7 \cdot 10^{-12} F$ which is the typical value in HFI.

Let's also consider a range of temperatures starting from the temperature of the plate (100mK for example) up to an arbitrary value. For each temperature we can calculate the impedance R_b of the bolometer and its total power using Eqs. 1 and 3. In this simulation we assume that the parameters of the bolometers (R_*, T_g, β, etc.....) are those of HFI.

If the optical background is constant in this run of simulations, the dissipated electrical power in the bolometer is:

$$W_{elec} = W_{tot} - W_{opt} \tag{22}$$

So, the r.m.s. Voltage at the ends of the bolometer is :

$$V_b = (R_b W_{elec})^{1/2} \tag{23}$$

and the r.m.s. bias current passing through the bolometer is:

$$I_b = \frac{V_b}{R_b} \tag{24}$$

In general for a quadripole we have:

$$F(V_b) = TF(\omega, R_b, C_p) \cdot F(V_0) \tag{25}$$

where F indicate the Fourier transform and $TF(\omega, R_b, C_p)$ is the transfer function of the quadripole. Using the quadripole obtained from Eq. 9, the module of the transfer function is :

$$|TF(\omega, R_b, C_p)| = \frac{R_b \omega C_b}{(1 + \omega^2 R_b^2 (C_b + C_p)^2)^{1/2}} \tag{26}$$

So, the r.m.s. input voltage is:

$$V_0 = \frac{V_b}{|TF(\omega, R_b, C_p)|} \tag{27}$$

In order to calculate the optical responsivity let us consider a small step in temperature for each bolometer. If we keep V_0 unchanged, the step in temperature is due to a change of the optical background that can be computed:

$$W_{opt1} = W_{tot1} - W_{elec1} \tag{28}$$

where W_{tot1} is calculated from the new temperature T_{b1} and W_{elec1} is derived from:

$$W_{elec1} = \frac{V_{b1}^2}{R_{b1}} \tag{29}$$

V_{b1} is equal to:

$$V_{b1} = V_0 \cdot |TF(\omega, R_{b1}, C_p)| \tag{30}$$

assuming that V_0 is not varying, and using the TF calculated from R_{b1}

The responsivity will be:

$$\Re = |\frac{V_{b1} - V_b}{W_{opt1} - W_{opt}}| \tag{31}$$

with the responsivity and NEP equations from the previous section, it is possible to calculate the total NEP

Appendix B: Computing the Responsivity with a Square Bias

With the same bias circuit (Fig. 1), it is possible to derive the performances of a REU in which a square wave voltage applied to the bolometer, as in HFI. Let us assume that if the REU is *balanced*, a perfect square wave bias is passing through the bolometer even in presence of a stray capacitance. In HFI this is achieved by using a triangular wave plus a square wave.

A square wave can be decomposed as:

$$V_b(\omega) = acos(\omega t) + \frac{a}{3}cos(3\omega t) + \frac{a}{5}cos(5\omega t) + ... =$$

$$= \sum_{n=0}^{\bar{n}} \frac{a}{2n+1} cos((2n+1)\omega t)$$

The r.m.s. V_b is equal to:

$$V_b = (\sum_{n=0}^{\bar{n}} (\frac{a}{\sqrt{2}(2n+1)})^2)^{1/2} \tag{32}$$

If the temperature of the bolometer is given and the optical power is constant we can calculate the r.m.s. V_b as we did for the sine bias case (Eq. 23 and Eq. 22). So we have:

$$a = (W_{elec} R_b)^{1/2} \cdot \sum_{n=0}^{\bar{n}} 2(2n+1)^2 \tag{33}$$

The r.m.s. bias current passing through the bolometer is:

$$I_b = \frac{V_b}{R_b} \tag{34}$$

Now let's derive the responsivity. As for the sine AC case, so we can calculate the R_{b1}, W_{tot1}, and the TF starting using a small step in temperature due to an incoming optical signal.

On the other hand we cannot derive the electrical power following the same logic: if we keep the same set up of the REU, after a small step in temperature the bias passing through the bolometer is not a square wave anymore so, the Eq. 32 is not applicable. We have to correct each term of the sum as follows:

$$W_{elect1} = \frac{a^2}{R_{b1}} \sum_{n=0}^{\bar{n}} 2(2n+1)^2 \cdot \Upsilon((2n+1)\omega, R_b, R_{b1}, C_p) \tag{35}$$

where

$$\Upsilon((2n+1)\omega, R_b, R_{b1}, C_p) = \frac{TF((2n+1)\cdot\omega, R_b, C_p)}{TF((2n+1)\cdot\omega, R_{b1}, C_p)} \tag{36}$$

References

1. J. J. A. Bock, Philip, L. Armus, J. Bally, D. Benford, A. Cooray, M. Devlin, S. Dodelson, D. Dowell, P. Goldsmith, S. Golwala, S. Hanany, M. Harwit, W. Holland, W. Holzapfel, Kenyon, Matt, K. Irwin, E. Komatsu, A. E. Lange, D. Leisawitz, A. Lee, B. Mason, J. Mather, H. Moseley, S. Meyer, S. Myers, H. Nguyen, V. Novosad, B. Sadoulet, G. Stacey, S. Staggs, P. Richards, G. Wilson, M. Yun, and J. Zmuidzinas, "Superconducting Detector Arrays for Far-Infrared to mm-Wave Astrophysics," in "astro2010: The Astronomy and Astrophysics Decadal Survey," , vol. 2010 of *ArXiv Astrophysics e-prints* (2009), pp. 45–+.
2. R. C. Jones, "The general theory of bolometer performance," Journal of the Optical Society of America (1917-1983) **43**, 1–+ (1953).

3. J. C. Mather, "Bolometer noise: nonequilibrium theory." Appl. Opt. **21**, 1125–1129 (1982).
4. J. C. Mather, "Electrical self-calibraion of nonideal bolometers," Appl. Opt. **23**, 3181–3183 (1984).
5. J. C. Mather, "Bolometers: ultimate sensitivity, optimization, and amplifier coupling," Appl. Opt. **23**, 584–588 (1984).
6. F. M. Rieke, A. E. Lange, J. W. Beeman, and E. E. Haller, "An AC bridge readout for bolometric detectors," IEEE Transactions on Nuclear Science **36**, 946–949 (1989).
7. T. Wilbanks, M. Devlin, A. E. Lange, J. W. Beeman, and S. Sato, "Improved low frequency stability of bolometric detectors," IEEE Transactions on Nuclear Science **37**, 566–572 (1990).
8. M. Devlin, A. E. Lange, T. Wilbanks, and S. Sato, "A dc-coupled, high sensitivity bolometric detector system for the Infrared Telescope in Space," IEEE Transactions on Nuclear Science **40**, 162–165 (1993).
9. S. Gaertner, A. Benoît, J.-M. Lamarre, M. Giard, J. Bret, J. Chabaud, F. Désert, J. Faure, G. Jegoudez, J. Landé, J. Leblanc, J. Lepeltier, J. Narbonne, M. Piat, R. Pons, G. Serra, and G. Simiand, "A new readout system for bolometers with improved low frequency stability," A&A Sup. Ser.**126**, 151–160 (1997).
10. E. Kreysa, F. Bertoldi, H. Gemuend, K. M. Menten, D. Muders, L. A. Reichertz, P. Schilke, R. Chini, R. Lemke, T. May, H. Meyer, and V. Zakosarenko, "LABOCA: a first generation bolometer camera for APEX," in "Society of Photo-Optical Instrumentation Engineers (SPIE) Conference Series," , vol. 4855 of *Society of Photo-Optical Instrumentation Engineers (SPIE) Conference Series*, T. G. Phillips & J. Zmuidzinas, ed. (2003), vol. 4855 of *Society of Photo-Optical Instrumentation Engineers (SPIE) Conference Series*, pp. 41–48.
11. J.-M. Lamarre et al., "Planck pre-launch status: the HFI instrument, from specifications to actual performance", in press, A&A (2010).
12. J. E. Vaillancourt, "Complex impedance as a diagnostic tool for characterizing thermal detectors," Review of Scientific Instruments **76**, 043107–+ (2005).
13. M. Piat, J.-P. Torre, E. Bréelle, A. Coulais, A. Woodcraft, W. Holmes, and R. Sudiwala, "Modeling of Planck-high frequency instrument bolometers using non-linear effects in the thermometers," Nuclear Instruments and Methods in Physics Research A **559**, 588–590 (2006).
14. S. Zwerdling, "A fast, high-responsivity bolometer detector for the very-far infrared," Infrared Physics **8**, 271–336 (1968).
15. J.-M. Lamarre, "Photon noise in photometric instruments at far-infrared and submillimeter wavelengths," Appl. Opt. **25**, 870–876 (1986).